CANADA

DEPARTMENT OF
ENERGY, MINES AND RESOURCES
MINES BRANCH
OTTAWA

ELECTRON-PROBE MICROANALYSIS OF ALLOYED GALVANIZED COATINGS

R. H. PALMER, H. R. THRESH AND J. J. SEBISTY

PHYSICAL METALLURGY DIVISION

Reprinted from the Proceedings of the Ninth International Galvanizing Conference, Dusseldorf, Germany, June, 1970.

Reprint Series RS 99

Price 25 cents

Available by mail from the Queen's Printer, Ottawa
and at the following Canadian Government bookshops

HALIFAX
1735 Barrington Street

MONTREAL
Æterna-Vie Building, 1182 St. Catherine St. West

OTTAWA
Daly Building, Corner Mackenzie and Rideau

TORONTO
221 Yonge Street

WINNIPEG
Mall Center Bldg., 499 Portage Avenue

VANCOUVER
657 Granville Street

or through your bookseller

Price 25 cents Catalogue No. M38-8/99

Price subject to change without notice

Queen's Printer for Canada
Ottawa, 1970

ELECTRON-PROBE MICROANALYSIS OF ALLOYED GALVANIZED COATINGS

by

R. H. PALMER, H. R. THRESH and J. J. SEBISTY
Department of Energy, Mines and Resources, Ottawa, Canada

INTRODUCTION

In earlier investigations into the effects of bath composition on the galvanizing characteristics of both mild and low-alloy high-strength steels[1, 2], it was established that several bath additions such as chromium, manganese, nickel, titanium and vanadium modified the coating structure and, in certain circumstances, effectively inhibited too rapid attack on the steel base by the molten zinc. It was considered that the observed changes in coating formation and structure might be explained by electron-probe microanalysis. Consequently, information was obtained on the distribution of the alloying additions and of the basic reactants - iron and zinc - in the coatings.

EXPERIMENTAL COATING PREPARATION

The galvanizing procedure has been described in an earlier paper[1]. The galvanizing baths, which were all saturated with iron (0.03% Fe) and alloyed with lead (1.0% Pb), were treated with individual additions of 0.2% Cr, 0.5% Mn, 0.2% Ni, 0.1% Ti and 0.2% V in the form of zinc-rich master alloys.

In some cases, a small aluminium addition was also made to suppress surface oxidation of the bath. The steel base was a low-alloy high-strength grade of normal galvanizing reactivity. The samples examined were galvanized at a temperature of 450°C (840°F) with an immersion time of 10 min. and were removed from the bath at a controlled withdrawal speed. In contrast, the 'control' (i.e. unalloyed) coating examined was formed by immersion for 20 min. at 450°C (840°F) of 24-gauge open-hearth rimmed steel. This difference in immersion time must be remembered when comparing microstructures.

METALLOGRAPHIC EXAMINATION

Metallographic specimens for microanalysis by the electron probe were mounted in copper-filled conducting diallylphthalate and polished down to a $\frac{1}{4}$ micron finish with non-aqueous media. The bevel through the zinc/iron alloy phases was held to within the depth of focus of the microprobe i.e. approximately 4 microns. After rinsing in ethyl alcohol and drying, the samples were etched in a picral solution.

The microstructures of the control coatings exhibited non-uniform but reciprocal growth of the zeta and delta-prime phases which varied slightly

from area to area. This had a corresponding effect on the thickness of the zinc layer as can be seen in Fig. 1. The alloyed coatings in most cases were distinguished by appreciable thinning of the zeta layer, thicker delta-prime formation, and by a significant improvement in the uniformity of all the individual layers (Figs. 2-5). The nickel- and titanium-containing coatings also exhibited gross intermetallic compounds at or near the zinc/zeta interface

ELECTRON MICROPROBE TECHNIQUE

Prior to examination in a Jeolco JXA3 microprobe, all specimens were oriented by means of microhardness indentations, repolished and coated with an evaporated layer of carbon to a thickness of between 50 and 75 Å. This treatment prevented the occurrence of occasional abnormalities in the X-ray data which could arise due to electron charging effects when the beam crossed grain boundaries in the columnar phases.

Preliminary experiments confirmed that this conductive coating did not interfere with the measurement of the X-ray intensities arising from the alloyed elements. Compositional variations through the alloy structure were determined by monitoring a maximum of two elements for each traverse. The X-ray spectrum was sampled every 10 sec., the specimen being driven under the 1-micron diameter beam at 2 microns/min. In this way, the variation of the monitored element was observed in detail on the pen recorder and the corresponding quantitative data from the scalers for the same time interval were accumulated on the typewriter print out. An excitation potential of 24 kV and current of 0.15 micro-amp gave adequate intensities of the $K\alpha_1$ X-ray lines employed for all elements.

By relating the measured element intensities of the alloy to the corresponding values of the pure standards, relative intensities were derived that were functions of the amount of the element present when the background correction and instrumental dead time had been accounted for. The intensity data were corrected for fluorescence and absorption effects in the respective matrices by a computer programme as proposed by Brown[3]. This procedure did not produce any major adjustments to the interpolated compositions as found from the raw data. More complete details on the probe procedure are given elsewhere[4].

RESULTS

The graphical data from the probe pen recorder were produced in terms of seconds (ordinate) versus total counts for a 10 sec. time interval (abscissa), this being converted to microns and percent respectively. Individual calculations were made, where applicable, for high, low and mean analyses within a phase but all individual point counts were not converted. However, a substantially accurate analysis at any point within the coating can be obtained by interpolation from the graphs in Figs. 1-5, provided that the finite diameter of the spot, and the fact that the count embraces the distance driven over the 10-sec. interval, are taken into account - particularly in the region of phase boundaries. Figs. 1-5 also contain the photomicrographs corresponding to the individual probe traces shown. Tables 1 and 2 contain the

calculated and corrected data of areas of particular interest to the investigation, these data being more comprehensive and more accurate than graphical interpolation.

Iron content

Without exception, the iron scan across every coating indicated that the iron content in the zeta phase increased slowly towards the zeta/delta-prime interface. At the interface there was a small but well-defined increase in iron content and thereafter the gradual rate was resumed through the palisade portion of the delta-prime phase (Figs. 1 and 2). A further step, and a more rapid increase in the iron gradient, marked the transition from palisade to compact delta-prime (Figs. 1 and 4).

The average iron content of 7.0% Fe for the zeta phase in all the coatings recorded in Table 1 was higher than the reported range of 6.0-6.2 $\pm$ 0.1% Fe for this layer under equilibrium conditions[5]. The average iron content of the palisade portion of the delta-prime phase was 8.8% Fe over a composition gradient of 7.4-9.8% Fe, as shown in Table 1. Similarly, the compact portion of the delta-prime phase averaged 11.3% Fe over a steeper iron gradient of 9.7-14.0% Fe. Thus the composition range found for the delta-prime phase as a whole was higher than the equilibrium data reported as 7.0-11.5 $\pm$ 0.5% Fe for this layer[5]. Hershman [6] previously established the existence of concentration gradients across the delta-prime palisade and coherent layers and the trace of the plotted iron results of Caloni and Ferrari[7] are also similar to the present findings. Cameron and Ormay[8] recorded lower numerical values for the overall iron content of the delta-prime phase but this was for high-aluminium coatings.

The electron-beam width of 1 micron prevented accurate determination of the iron content of the thin gamma phase.

Zinc content

As is indicated, for example, in the probe trace of Fig. 1, the zinc and iron contents were largely complementary in that the zinc content varied inversely as the iron content.

Lead content

The microprobe showed that in both the control and alloyed coatings, lead was present as randomly scattered globules dispersed throughout the zinc layer.

Manganese content

The variations in iron and manganese concentrations across the manganese-containing coating are shown in Fig. 2. Manganese in the zinc layer was relatively constant but increased rapidly to a maximum at about 0.9% (Table 2) at the outer edge of the zeta phase. Across the zeta phase, a declining composition gradient was indicated with manganese decreasing to 0.6%. This was followed by a sudden drop at the zeta/delta-prime interface and a further

continuous decrease through the delta-prime phase until a minimum was reached near the gamma boundary. Beyond this minimum in the delta prime, there was a sharp rise in manganese in the gamma phase. This may have been derived from outward diffusion of manganese from the steel base but was more likely due to the probe spot simultaneously sampling both the gamma and the steel base.

It would appear, therefore, that the zeta phase has a high affinity for manganese. The minimum manganese content located in the delta-prime phase also indicated that the manganese in the coating was derived primarily from the galvanizing bath (0.5% Mn) and not the steel substrate.

Nickel content

A small amount of nickel was indicated for the zinc layer but, as shown by the nickel trace in Fig. 3, the nickel content increased drastically within the intermetallic compounds, most of which were located at or near the zinc/zeta interface. Within the alloy layers, nickel was concentrated at the outer edge of the thin zeta phase and decreased rapidly to zero, i.e. the background count, within this phase. Thus, nickel penetrated the alloy layers of the coating less deeply than did manganese.

The composition of the alloy-rich intermetallic compounds found in the nickel and other alloyed coatings was studied in more detail. These were found to be of ternary composition and, in the case of the Zn-Fe-Ni compound, the iron content was about 4.6% as shown by the four determinations in Table 2. It should be noted that the nickel content is about 20 times greater than that of the galvanizing bath (0.2% Ni). From the probe results and the distribution of the compounds in the microstructure, it would appear that the Zn-Fe-Ni particles were produced at or near the zinc/zeta interface, and approximated to a nickel-enriched form of the zeta phase. Presumably, the presence of the ternary compounds at the interface could form both a mechanical and a diffusion barrier reducing the supply of zinc to the underlying layers.

As noted, there was negligible nickel in the delta-prime or gamma phases.

Titanium content

Titanium was also primarily located in ternary intermetallic compounds floating in the zinc layer (Fig. 4). As shown in Table 2, the average iron content was again about 4.5% Fe and the titanium level was about 1.7%. This titanium value is about 20 times higher than the bath composition (0.1% Ti). The ternary compound had maximum core concentrations of 2.9% Ti and 7.1% Fe (Table 2). The latter approximates to the iron concentration of the zeta phase.

Vanadium content

The bath containing 0.2% V produced a coating with a maximum vanadium content of 1% concentrated at the outer edge of the zeta phase. This distribution is clearly shown by the photomicrograph and chart in Fig. 5. The vanadium

content decreased rapidly with distance from the zinc/zeta interface to zero or background count within the zeta phase. Again, the vanadium appeared to be forming zinc-rich intermetallic compounds at the interface.

A Mines Branch electron-probe investigation on vanadium-containing dross samples[9] revealed floating ternary Zn-1.7%V-6.5% Fe compounds which were apparently nucleated as a by-product of the galvanizing reaction. The iron content suggests they were a ternary modification of the zeta phase although the hexagonal form of the particles was not compatible with the monoclinic structure of zeta. The ternary material in the present work had lower vanadium and iron contents (Table 2), but presumarly represented compound formation from the same source.

The vanadium content indicated for the delta-prime and gamma phases in Fig. 5 was simply the background count and both these phases were substantially free from vanadium.

Chromium content

Although the chromium content of the coatings prepared in the galvanizing bath was 0.2%, this was not detected by the electron probe. Metallographically, chromium appeared to alter the zinc/iron coating structure similarly to the vanadium addition described above.

SUMMARY AND DISCUSSION

In the past, there has always been an element of speculation when interpreting microstructures in terms of equilibrium diagrams, since the system was obviously not in equilibrium. However, the microprobe has enabled the relationships between the observed metallographic structure, the published equilibrium diagram and the chemical composition to be established with considerable confidence.

The iron scans across the various coatings indicated that the iron contents in the zeta and delta-prime phases were higher than those reported under equilibrium conditions[5]. The iron content increased continuously towards the steel base, this increase being slight through the zeta and palisade delta-prime and progressively steeper through the compact delta-prime and gamma phases. The interface between each of these regions was marked by a definite step in the iron content curve. These results are similar to those of Hershman[6] and support his conclusion that the compact and palisade regions of the delta-prime are distinct layers having different diffusion coefficients. Further evidence of the two separate structures in the delta phase was obtained in related studies on heat-treated conventional galvanized coatings[10].

The curves established for the zinc contents in the various phases were the inverse of the iron contents.

Of the alloying elements added, manganese was unique in that it was incorporated into the zinc/iron alloy layers in some depth, with a heavy concentration throughout the zeta layer. Metallographically, the effect of man-

ganese was to produce a uniform and compact zeta layer, and a uniform delta-prime layer. Considering that the delta is growing principally by absorbing the zeta phase, manganese may have modified the reaction, either by reducing the diffusion of zinc downwards through the zeta layer, or by increasing the outward diffusion of iron through the delta prime. Alternatively, manganese may have substituted for iron to increase the 'effective' iron content of the various phases but the probe traces of iron in Fig. 2 show that this can be discounted. It also shows that despite the presence of considerable manganese in the zeta phase, the composition limits for iron over which this phase was stable were apparently not affected. The normal thickness of the zeta phase suggests that this layer was not eroded away abnormally by the manganese-containing bath to form intermetallics at the zinc/zeta interface, or excessive dross particles to contaminate the galvanizing bath. Coupled with the relative low cost and ease of alloying of this element, these various factors suggest that manganese might have broader applications in general galvanizing whenever the structure or properties of the zeta phase are important e. g. long-term corrosion.

The nickel, titanium and vanadium additions, which earlier work[2] showed were the most effective inhibitors of excessive zinc/iron alloy growth on reactive steels, produced similar structures and probe traces. These alloying elements were primarily concentrated in the form of ternary compounds at the outer edge of the zeta phase, or in a band in the zinc adjacent to the zeta. The distribution of these phases, their high iron content, and the fact that the zeta phase was very thin, all suggest that the ternary compounds were formed at the zinc/zeta boundary, either epitaxially with the zeta or nucleated from the molten zinc. If it is considered that they were formed as an extension of the zeta and bonded to it, this would account for the thin zeta phase and the fact that the compounds were not observed in the bath to any great extent. Also, bonded compounds might be expected to form both a diffusion barrier and a mechanical barrier reducing the amount of zinc in contact with the zeta. In turn, either or both these effects would be expected to reduce the thickness of the zeta layer (in favour of delta) and to reduce the overall thickness of the alloy layers by restricting the supply of zinc. In this regard, it might be mentioned that the vanadium compounds were smaller, appeared to be more intimately bonded to the zeta phase and that vanadium was, in general, the most effective element in inhibiting excessive reaction rates in the case of more reactive galvanizing grades of steel containing silicon and phosphorus.

It could also be speculated that nickel, titanium and vanadium have a higher affinity for iron than for zinc and could react initially with the steel base to form binary iron-base alloys. If this were true, the effect of these additions would be analgous to the inhibiting effect of aluminium which forms an Fe_2Al_5 layer at the steel interface.

Although the chromium content was not measurable by the electron probe, metallographically the chromium addition to the bath appeared to inhibit the reaction and alter the coatings structurally in a similar manner to the vanadium.

ACKNOWLEDGEMENTS

The authors are indebted to the Director of the Mines Branch, Department of

Energy, Mines and Resources, for permission to publish the paper, and to the Canadian Zinc and Lead Research Committee and the International Lead Zinc Research Organization Inc., for their cooperation.

REFERENCES

1. Sebisty, J.J. and Palmer, R.H. Hot dip galvanizing with less common bath additions. Proc. Seventh Intern. Conf. on Hot Dip Galvanizing, Paris, 1964. Oxford, Pergamon P., 1967, pp. 235-265.

2. Sebisty, J.J. and Palmer R.H. Galvanizing of low-alloy high-strength steels. Proc. Eighth Intern. Conf. on Hot Dip Galvanizing, London, 1967. London, Industrial Newspapers Ltd., 1969. pp. 30-58.

3. Brown, J.J. A comprehensive computer programme for electron-probe microanalysis. Anal. Chem., 1966, 38 (7), 890

4. Palmer, R.H. and Thresh, H.R. Electron-probe microanalysis of alloyed galvanized coatings. Ottawa, Department of Energy, Mines & Resources, Mines Branch, July 1969. Physical Metallurgy Division internal report PM-R-69-12.

5. Raynor, G.V. The equilibrium diagram of the system iron-zinc. London, Institute of Metals, 1951. Annotated equilibrium diagram series No. 8.

6. Hershman, A.A. Alloy formation in hot dip galvanizing: some current experiments. Proc. Seventh Intern. Conf. on Hot Dip Galvanizing, Paris, 1964, Oxford, Pergman P., 1967. pp. 189-208.

7. Caloni, O. and Ferrari, A. Application of a microanalyser with an electronic probe to the study of protective coatings. Atti Not. Assoc. Ital. Met., 1967, 22 (2/3), 45-46.

8. Cameron, D.I. and Ormay, M.K. The effects of agitation, cooling and aluminium on the alloying in hot dipping in zinc. Proc. Sixth Intern. Conf. on Hot Dip Galvanizing, Interlaken, 1961. London, Zinc Development Association. pp. 276-316.

9. Sebisty, J.J. and Palmer, R.H. Electron-probe microanalysis of vanadium-containing galvanizing samples. Ottawa, Department of Energy, Mines & Resources, Mines Branch, June 1969. Investigation report IR-69-44.

10. Palmer, R.H. and Thresh, H.R. Electron-probe microanalysis of heat-treated conventional galvanized coatings. Ottawa, Department of Energy, Mines & Resources, Mines Branch, June 1969. Physical Metallurgy Division internal report PM-R-69-14.

TABLE 1 - IRON CONTENTS OF DELTA-PRIME AND ZETA PHASES CORRECTED FOR BACKGROUND, DEAD TIME, FLUORESCENCE AND ABSORPTION

Type of coating	Traverse No.	Elements analysed	Iron content* of delta-prime phase (%)		Iron content of zeta phase (%)
			Compact portion	Palisade portion	
Control	2	Fe-Zn	11.6 (13.3-10.1)	8.9 (9.6-7.8)	6.9
	3	Fe-Zn	11.4 (13.1-10.0)	8.7 (9.3-7.7)	6.9
Vanadium-containing	4	Fe-V	11.6 (14.0-10.0)	9.0 (9.8-8.1)	7.1
	6	Fe-V	11.3 (13.5- 9.9)	8.8 (9.6-7.9)	7.0
Chromium-containing	1	Fe-Cr	11.6 (13.2-10.0)	8.8 (9.5-7.4)	7.0
Manganese-containing	1	Fe-Mn	10.8 (12.4- 9.8)	9.0 (9.5-7.9)	7.0
	2	Fe-Zn	11.0 (12.6- 9.9)	8.8 (9.5-7.7)	6.9
	3	Fe-Mn	11.2 (12.3- 9.9)	8.8 (9.5-7.7)	6.8
Nickel-containing	1	Fe-Ni	10.8 (12.6- 9.8)	8.8 (9.5-7.9)	7.2
	2	Fe-Zn	11.4 (13.5-10.0)	8.8 (9.5-7.6)	7.4
	3	Fe-Ni	11.1 (13.7- 9.9)	8.8 (9.5-7.8)	7.3
	4	Fe-Ni	10.9 (14.0- 9.7)	9.0 (9.5-7.5)	7.2
	5	Fe-Zn	11.3 (13.6- 9.8)	9.0 (9.5-7.7)	7.1
Titanium-containing	1	Fe-Ti	11.4 (12.7-10.0)	8.0 (9.0-7.4)	6.9
**			11.3 (13.2- 9.9)	8.8 (9.5-7.7)	7.0
***			14.0 - 9.7	9.8 - 7.4	

* Compositional range in brackets.
** Average of 14 separate traverses listed.
*** Individual maxima and minima.

TABLE 2 - MAXIMUM CONCENTRATION OF BATH ALLOYING ADDITIONS CORRECTED FOR BACKGROUND, DEAD TIME, FLUORESCENCE AND ABSORPTION

Type of coating	Traverse No.	Concentration (%)					
		Fe	Zn	Mn	Ni	Ti	V
Manganese-containing	1	5.4	-	0.9	-	-	-
	3	6.3	-	0.9	-	-	-
Nickel-containing	1	4.8	-	-	4.7	-	-
	2	4.7	89.2	-	-	-	-
	3	4.4	-	-	5.1	-	-
	4	4.5	-	-	4.2	-	-
Titanium-containing	1	4.4	-	-	-	1.7	-
	1	7.1*	-	-	-	2.9*	-
Vanadium-containing	4	1.4	-	-	-	-	0.9
	5	-	93.9	-	-	-	1.0
	6	3.8	-	-	-	-	1.0
	7	-	93.9	-	-	-	0.6

* Central core of intermetallic compound.

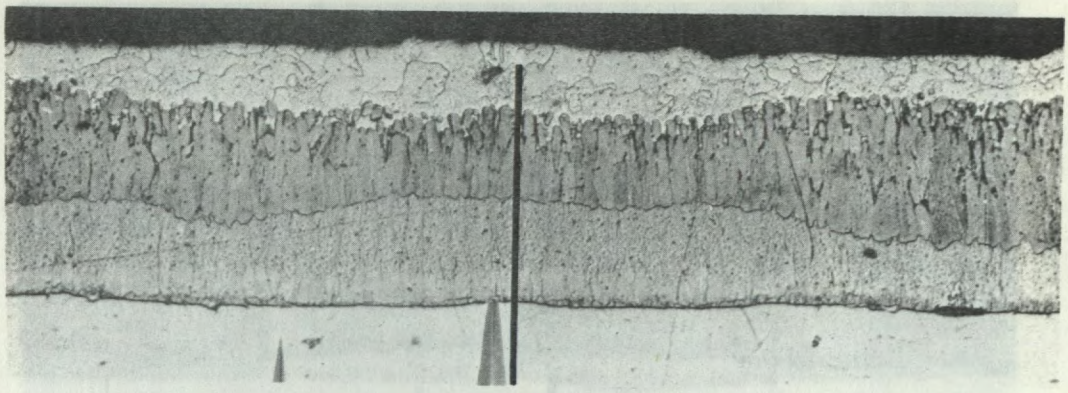

(a) Photomicrograph showing traverse of electron beam, X500.

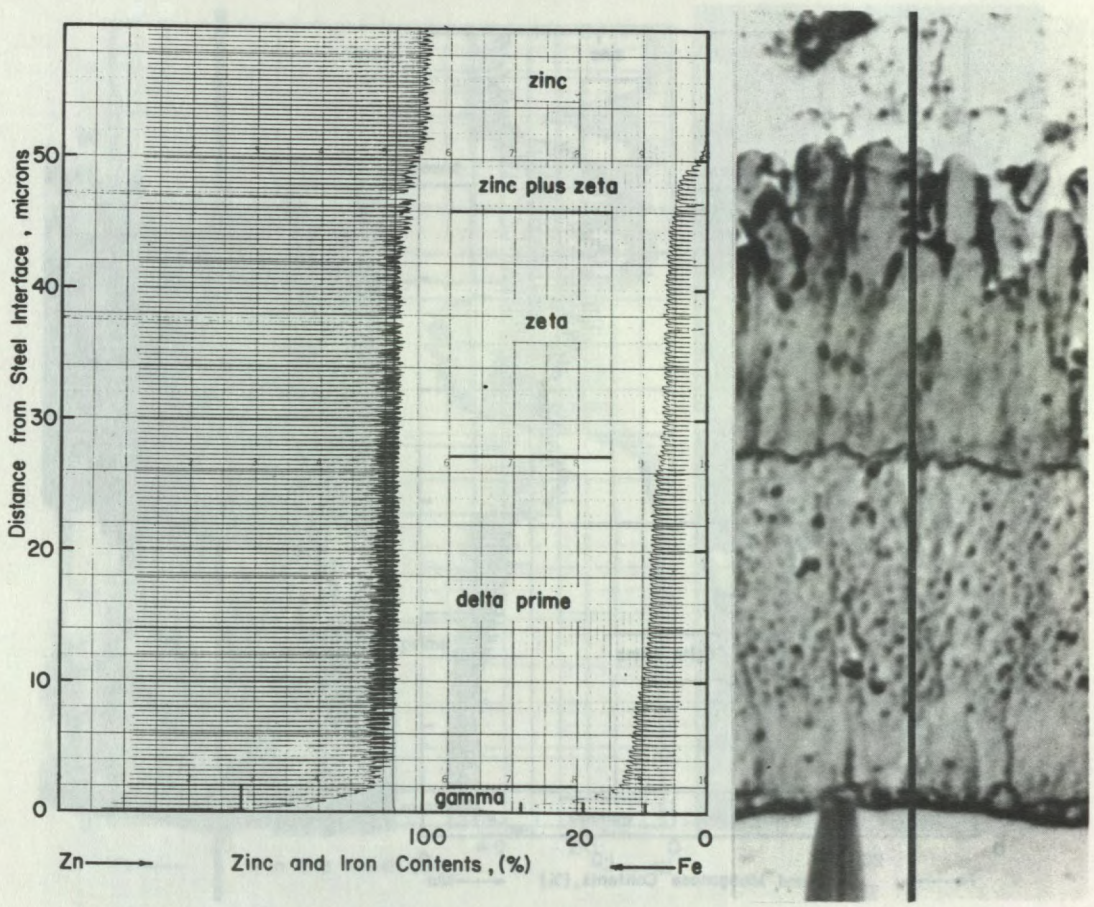

(b) Charted Zn and Fe data combined with enlargement of (a)

Figure 1. Electron-probe microanalysis of conventional "control" coating formed in 20 minutes at 450°C (840°F).

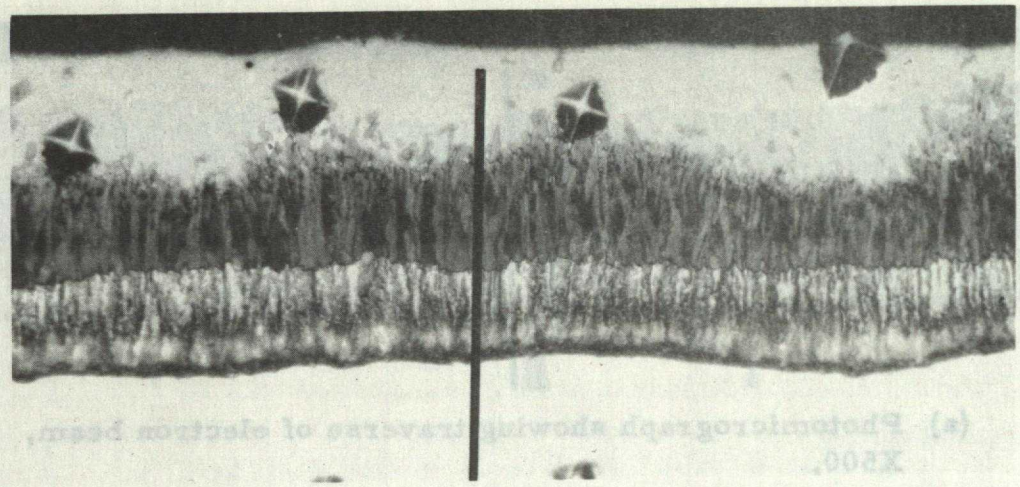

(a) Photomicrograph showing traverse of electron beam, X500.

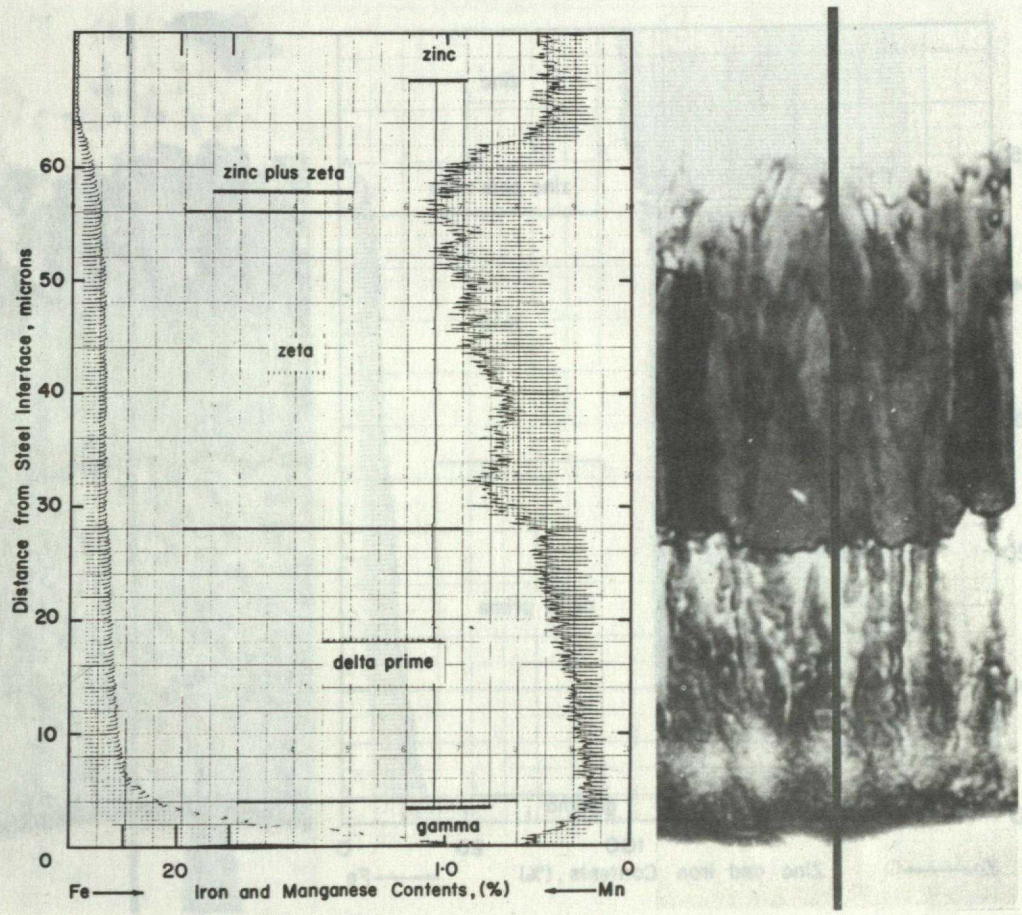

(b) Charted Fe and Mn data combined with enlargement of (a).

Figure 2. Electron-probe microanalysis of manganese-containing galvanized coating formed in 10 minutes at 450°C (840°F).

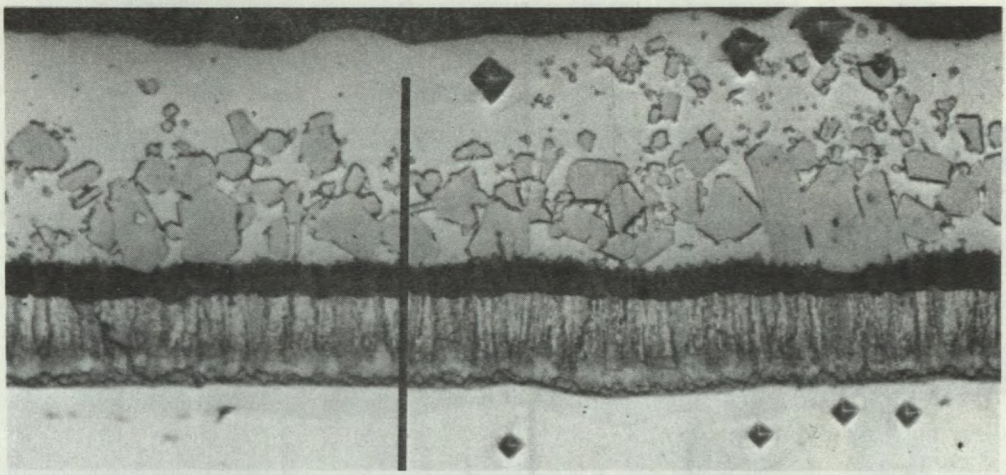

(a) Photomicrograph showing traverse of electron beam, X500.

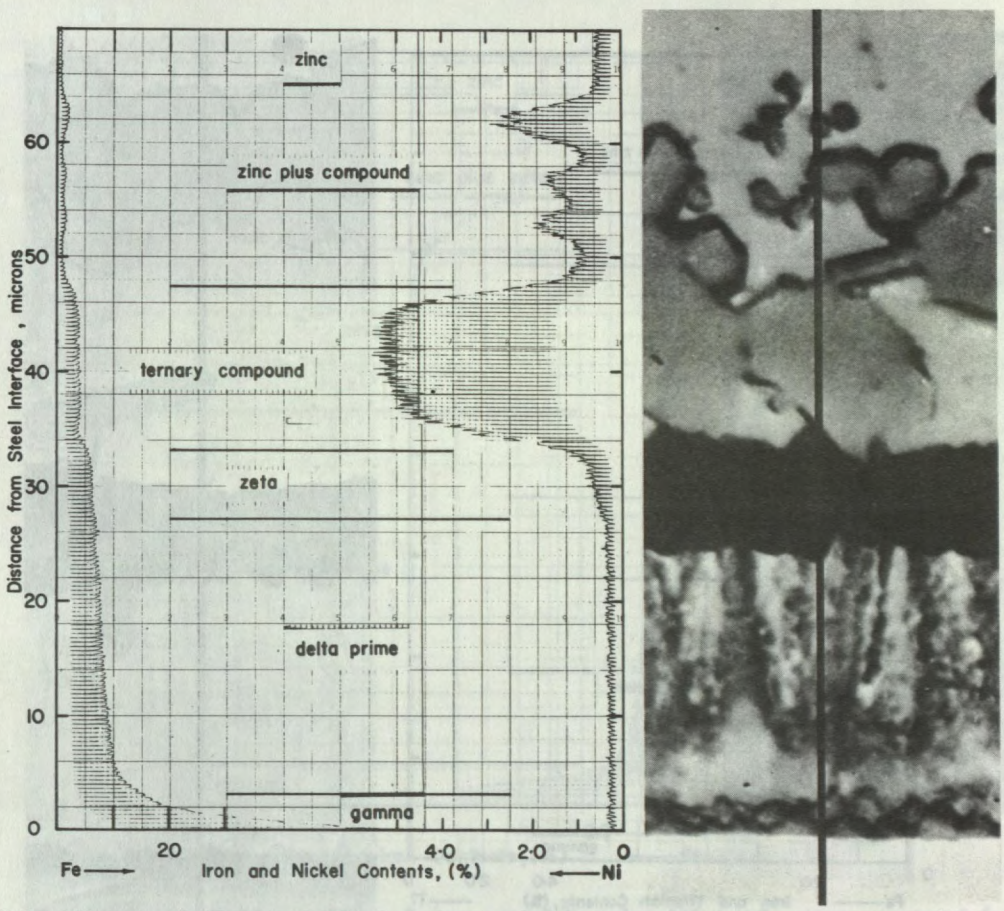

(b) Charted Fe and Ni data combined with enlargement of (a).

Figure 3. Electron-probe microanalysis of nickel-containing galvanized coating formed in 10 minutes at 450°C (840°F).

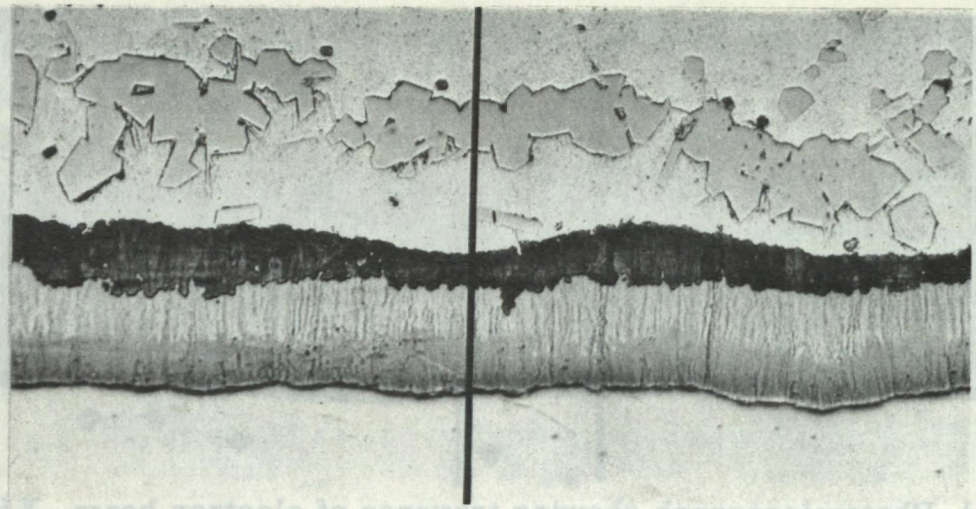

(a) Photomicrograph showing traverse of electron beam, X500.

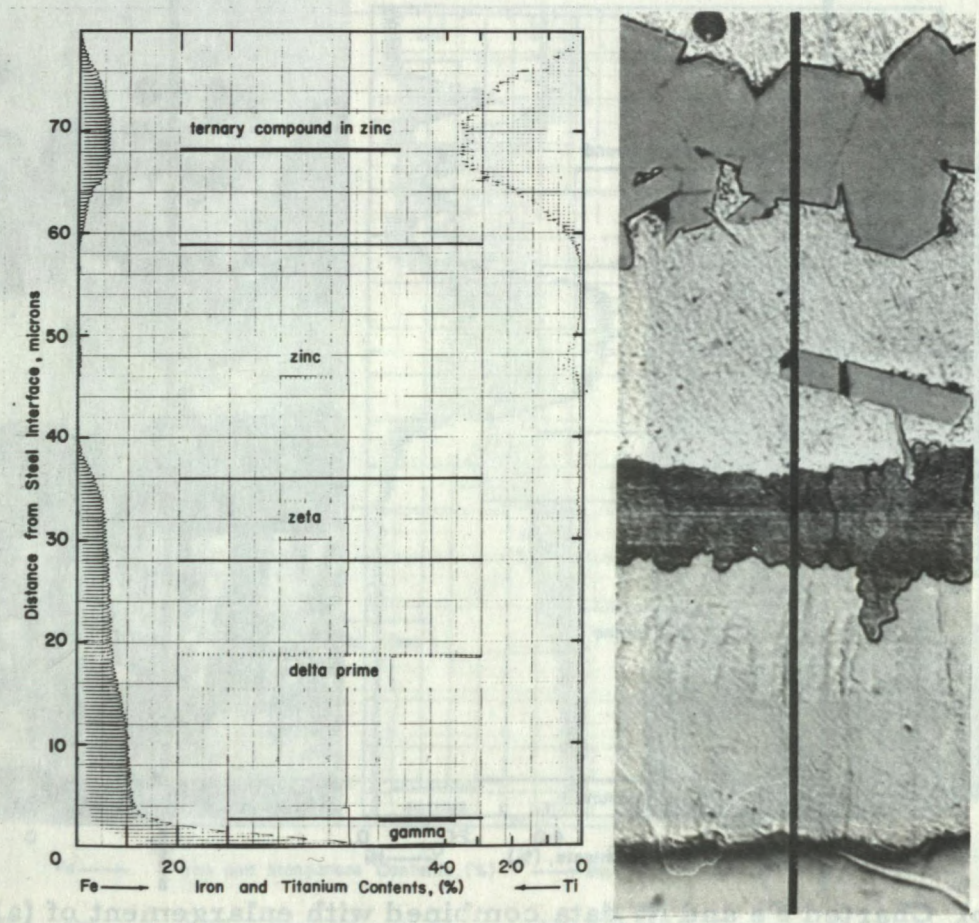

(b) Charted Fe and Ti data combined with enlargement of (a).

Figure 4. Electron-probe microanalysis of titanium-containing galvanized coating formed in 10 minutes at 450°C (840°F).

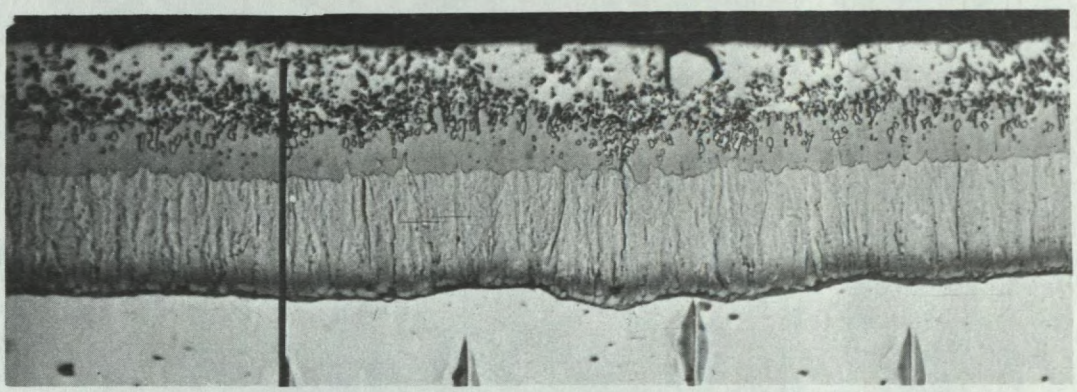

(a) Photomicrograph showing traverse of electron beam, X500.

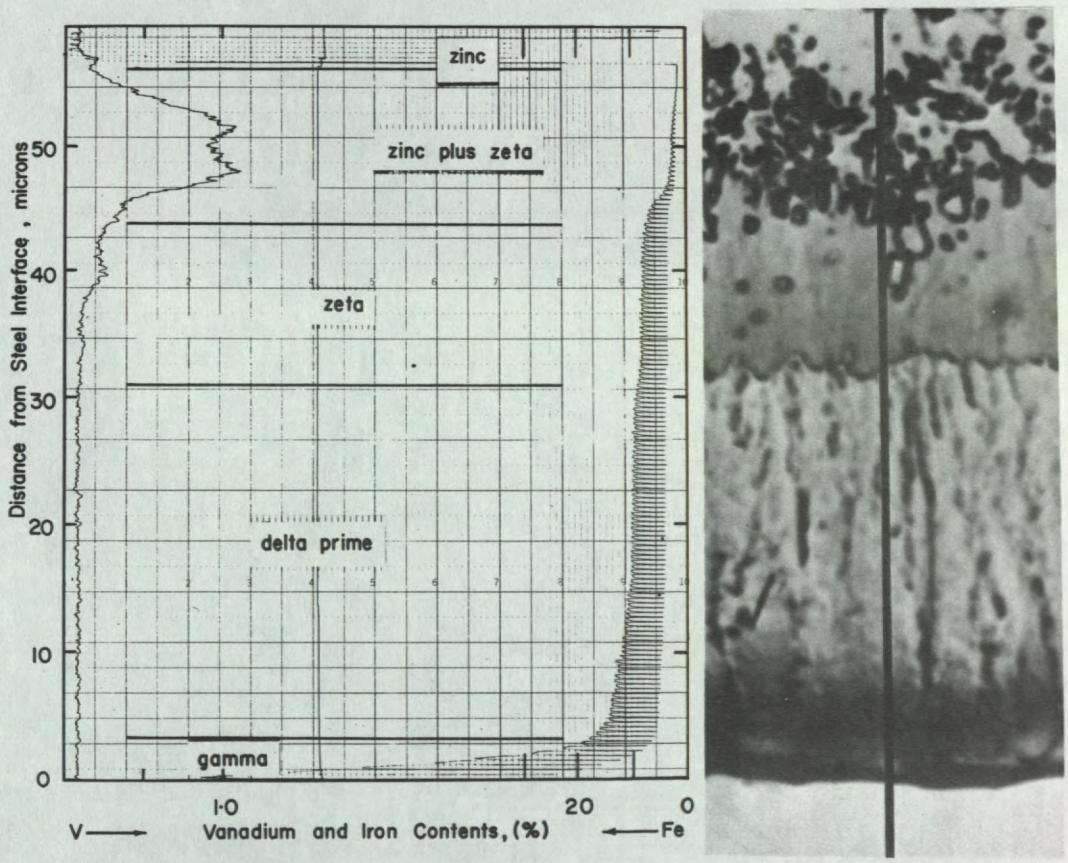

(b) Charted V and Fe data combined with enlargement of (a).

Figure 5. Electron-probe microanalysis of vanadium-containing galvanized coating formed in 10 minutes at 450°C (840°F).